

Article

Understanding Binding of Quaternary Ammonium Compounds with Cellulose-Based Fibers and Wipes for Renewable and Sustainable Hygiene Options

Monika Mali ^{1,2}, Khandoker Samaher Salem ^{2,3}, Roman Sarder ², Sachin Agate ², Kavita Mathur ⁴ 
and Lokendra Pal ^{2,*} 

¹ Department of Textile Engineering, Chemistry and Sciences, Wilson College of Textiles, North Carolina State University, Raleigh, NC 27606-8301, USA; monika.mali31@gmail.com

² Department of Forest Biomaterials, College of Natural Resources, North Carolina State University, 2820 Faucette Drive, Raleigh, NC 27695-8005, USA; ksalem@ncsu.edu (K.S.S.)

³ Department of Applied Chemistry and Chemical Engineering, University of Dhaka, Dhaka 1000, Bangladesh

⁴ Department of Textile and Apparel, Technology and Management, Wilson College of Textiles, North Carolina State University, Raleigh, NC 27606-8301, USA

* Correspondence: lpal@ncsu.edu

Abstract: Cellulose-based fibers are desirable materials for nonwoven wipes for their good absorbency, strength, cleaning, and biodegradable properties. However, quaternary ammonium compounds (QACs), being cationic in nature, show electrostatic interactions with anionic cellulosic fibers, reducing the available QACs to efficiently clean surfaces. This research presents sustainable alternative fibers that show better controlled exhaustion than commercial wipes and textile fibers. Textile and lignocellulosic fibers were prepared, soaked in QAC, and a UV-vis spectrophotometer was used to measure their exhaustion percentages. Factors such as immersion time and concentration of the disinfectant were also investigated, which affect the rate of exhaustion of the disinfectant from the fibers. A higher immersion time resulted in better exhaustion, whereas the total exhaustion decreased with an increase in the initial concentration of the disinfectant. The exhaustion of benzalkonium chloride (BAC) from the commercial wipes was also investigated at different immersion times and BAC concentrations. It was found that the wood and non-wood fibers showed more controlled exhaustion than the textile fibers and commercial wipes, and could be considered an alternative option for renewable and sustainable wipes and hygiene products.

Keywords: quaternary ammonium compounds (QACs); cellulosic fibers; release and binding disinfectants; wipes; charge content; health and hygiene products



Citation: Mali, M.; Salem, K.S.; Sarder, R.; Agate, S.; Mathur, K.; Pal, L. Understanding Binding of Quaternary Ammonium Compounds with Cellulose-Based Fibers and Wipes for Renewable and Sustainable Hygiene Options. *Sustainability* **2024**, *16*, 1586. <https://doi.org/10.3390/su16041586>

Academic Editor: Hailong Yu

Received: 31 October 2023

Revised: 2 February 2024

Accepted: 6 February 2024

Published: 14 February 2024



Copyright: © 2024 by the authors. Licensee MDPI, Basel, Switzerland. This article is an open access article distributed under the terms and conditions of the Creative Commons Attribution (CC BY) license (<https://creativecommons.org/licenses/by/4.0/>).

1. Introduction

The rapid growth in the production of disposable nonwoven wipes is attributed to the good physical properties of nonwoven fabrics, such as their non-directional high tensile strength, high absorbency, capacity to retain their original shape, and their single-use nature [1]. Additionally, the production of nonwoven fabrics is inexpensive and can be produced in large volumes, which leads to many new consumer products, such as floor cleaning, hard surface disinfecting wipes [2]. Moreover, according to reports on sustainable nonwoven fabrics, disinfecting and other nonwoven wipes are essential tools to restrict the spread of many infectious and contagious diseases, such as coronavirus [3]. Therefore, the total market value of nonwoven wipes is expected to continue to expand at a compound annual growth rate of 5.8% to reach \$26.07 billion in 2025 [4]. However, most raw materials used to produce nonwoven fabrics are non-biodegradable synthetic materials like polypropylene and polyester, because they are relatively inexpensive and have attractive aesthetic and mechanical properties [2,5]. Thus, a large amount of non-biodegradable

nonwoven material is thrown away after single-use or non-durable applications, which increases the volume of municipal solid waste and poses a challenge to landfilling disposal systems [6–9].

With consumer preferences shifting away from petroleum-based products to more sustainable options, cellulose-based nonwoven wipes could be a sustainable alternative since they are biodegradable, recyclable, and have good mechanical and aesthetic properties [10,11]. However, the cellulosic materials used in different hygiene products [12] as sustainable biomaterials for their functionality of being tuned by substituting the cellulose hydroxyls with other functional groups according to the application [10,13], have been inadequately utilized for nonwoven wipes production, where viscose or regenerated cellulose are used solely or mixed with synthetic fibers at different percentages [14]. The limited use of cellulosic materials is due to the use of the quaternary ammonium surfactants to disinfect hard surfaces, which readily adsorb onto the fibers, and are thus not released onto the contaminated surface [15,16]. Quaternary ammonium compounds (QACs) are compounds with a general structure consisting of a central nitrogen with four alkyl/aryl groups attached with covalent bonds [17,18]. The properties of these compounds depend upon the attached alkyl groups (R groups). The negatively charged anion portion (X^-), which is usually chlorine or bromine, is linked to nitrogen to form QAC salt. Varying the attached alkyl group (numbers of carbon atoms, branched chains, and aromatic rings) can affect the antimicrobial activity of the quats in terms of dose and action against different groups of microorganisms [19]. QACs' positively charged cations' mode of action is related to their attraction to negatively charged materials such as bacterial protein. Electrostatic interaction between the negatively charged bacterial cellular membrane and the positively charged QAC head is followed by permeation of the QAC side chains into the intramembrane region, ultimately leading to leakage of cytoplasmic material and cellular lysis [20,21]. As shown in Figure 1, during the inactivation of bacterial cells, the quaternary ammonium group remains intact and retains its antimicrobial ability. QACs provide broad-spectrum activity against bacteria, fungi, algae, and certain viruses, as they act on the membrane structure. However, they are more active on Gram-positive than Gram-negative bacteria because Gram-positive bacteria have only a single-layer membrane, whereas Gram-negative bacteria are encapsulated in two cellular membranes [22–24].

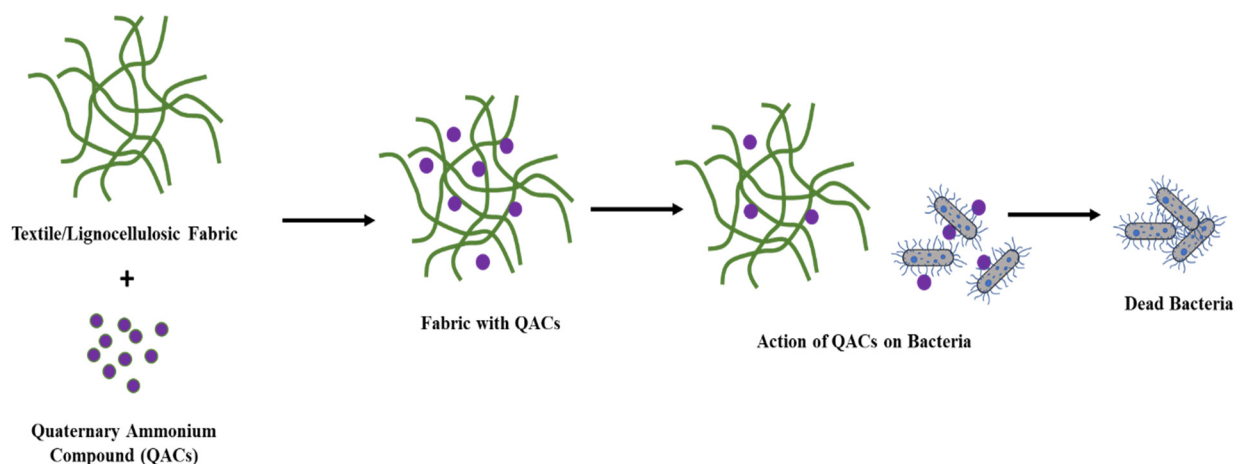


Figure 1. QACs mechanism of action on bacteria.

The cellulose-based material generates an anionic charge when immersed in water, since it possesses a negative charge (carboxyl group) due to the presence of ionizing groups on the cellulose originating from cell wall constituents (resins, fatty acids, carboxylic acid groups of the hemicelluloses, and lignin's phenolic groups) during pulping and bleaching [25]; furthermore, QACs are cationic, and become attached to the fiber surface through electrostatic interactions with anionic residues bonded covalently to the polymer/fiber

structure [26]. This interaction results in quat depletion from the disinfecting solution, effectively lowering the concentration of the QACs from the disinfecting solution, and lowering the quat concentration to a level that is no longer efficacious against the target microorganism [15,27–29]. Thus, different approaches have been investigated, including chemical surface modification, chemical blocking, co-formulation, and changing the substrate surface properties by coating and optimizing the chemical and physical properties of disinfectant solutions to reduce QAC bonding with cellulosic materials, which would result in improved disinfecting [30,31]. However, the effects of different wood and non-wood feedstocks on the interactions between QAC and cellulosic fibers have not been investigated thoroughly to understand the binding mechanism and strategies to avoid it. This article reports on BAC exhaustion experiments with various cellulose-based natural and regenerated fibers as well as commercially available wipe samples, which were conducted to understand the interaction of BAC with different fiber types, such as hardwood (southern bleached hardwood kraft, SBHK), softwood (southern bleached softwood kraft, SBSK), bleached eucalyptus (BEK), hemp kraft (HK), hemp carbonate (HC), and some market pulp. Further, the exhaustion of benzalkonium chloride (BAC) was studied under different conditions, such as the solution concentration, time of exhaustion, and types of fibers.

2. Experimental Section

2.1. Materials

Cellulosic, regenerated cellulosic, and synthetic fibers were used to perform the experiments. Southern bleached hardwood kraft (SBHK), northern bleached softwood kraft (NBSK), and bleached eucalyptus kraft (BEK) pulps were obtained from local pulp and paper mills. Hemp kraft (HK) and hemp carbonate (HC) were prepared in the lab from dew-retted and decorticated Futura 75 cultivar hemp hurds procured from the Netherlands. Commercial wipes were purchased from Contec Inc., USA. Different chemicals, such as 50% *w/w* benzalkonium chloride aqueous solution, polyelectrolyte solutions, anionic polyelectrolyte PVS- Na 0.001 N, and cationic polyelectrolyte 0.001 N were sourced from Fisher Scientific, Hampton, NH, USA.

2.2. Methodology

- **Characterization of Fibers:** The fiber length (*lw*), fine contents, and other physical properties of the different wood and non-wood fibers were determined using a high-resolution fiber quality analyzer: HiRes FQA, OpTest Equipment Inc (Hawkesbury, ON, Canada). Before testing, the fiber quality analysis was calibrated and used according to the manufacturer's specifications [25]. The textile fiber's staple length was determined as per ASTS D5103 (performed manually), and its linear density was determined as per ASTM standard test method D1577 using a vibroscope.
- **Characterization of Wipes:** The basis weight of the wipes (in GSM) was calculated according to TAPPI standard T 410, and the thickness was measured using a caliper T 411. The absorbent capacity of the wipes was taken from the datasheet provided by the manufacturer (tested as per IEST-RP-CC004.3 sec.8.1).

Surface Charge Density: The surface charge density of all the fibers were measured using an AFG charge analyzer. A volume of 10 mL of fiber suspension from the prepared stock solution was poured into the sample holder of the measuring device. The fibers have anionic charges when immersed in water, so the titrant was cationic. The titration speed and volume were preset as a volume increment of 50 μ L after every four seconds. Titration was continued until the streaming potential became zero. For every fiber, the experiment was repeated four times, and the average value was noted. The data collected using AFG software version 3.04 included values for the titrant volume demand (mL) and surface charge density in (μ equivalent/L) and streaming potential with every volume dosage.

Fourier Transform Infrared Spectroscopy (FTIR): FTIR spectra of the samples were observed using a PerkinElmer Spectrum One FTIR spectrometer. Attenuated total reflectance

(ATR) data were recorded between 4000 and 500 cm^{-1} with a resolution of 4 cm^{-1} , with 32 scans for each sample, and the baseline was adjusted as well.

X-ray Diffraction (XRD) Analysis: A Rigaku SmartLab X-ray diffractometer was used and operated at 45 kV and 40 mA with Ni-filtered CuK radiation to determine the crystallinity indices of the differentially processed bleached and unbleached wood, non-wood, and textile fibers. X-ray diffractograms were captured at a rate of $0.02^\circ \text{ s}^{-1}$ over a 2-scan range of $5\text{--}60^\circ$. The diffraction data collected for each sample were deconvoluted to calculate the area corresponding to crystalline and amorphous peaks; thus, the crystallinity index was calculated following the peak deconvolution method [32].

Scanning Electron Microscopy (SEM): Morphological characterizations of the samples were carried out using a Hitachi S3200N variable pressure scanning electron microscope (VPSEM). The samples were dried overnight to completely remove moisture. All of the samples were sputter coated with AuPd for 4 min, and images were taken at 2 kV at the same magnifications.

Exhaustion of Benzalkonium chloride (BAC) Solution from Fibers and Wipes: A mass of 20 milligrams of oven-dried fiber sample was placed in a flask containing 20 mL of benzalkonium chloride (BAC) solution with two different concentrations of 0.625 g/L and 1.25 g/L, and for three time intervals (5, 30, and 60 min). After each time interval, the wet sample was centrifuged at 0.9 relative centrifugal force (rcf) for 1 min to remove the BAC solution from the fibers and wipes. The solution from the top of the vial was taken using a microfilter syringe (0.45 micrometer) to avoid small fiber particles in the test solution. The absorbance of the filtered solution was measured using a UV spectrophotometer (Perkin Elmer Lambda max) at 262 nm. The lambda max and calibration curve (Figure 2) for benzalkonium chloride were found using serial dilution at the beginning of the experiment.

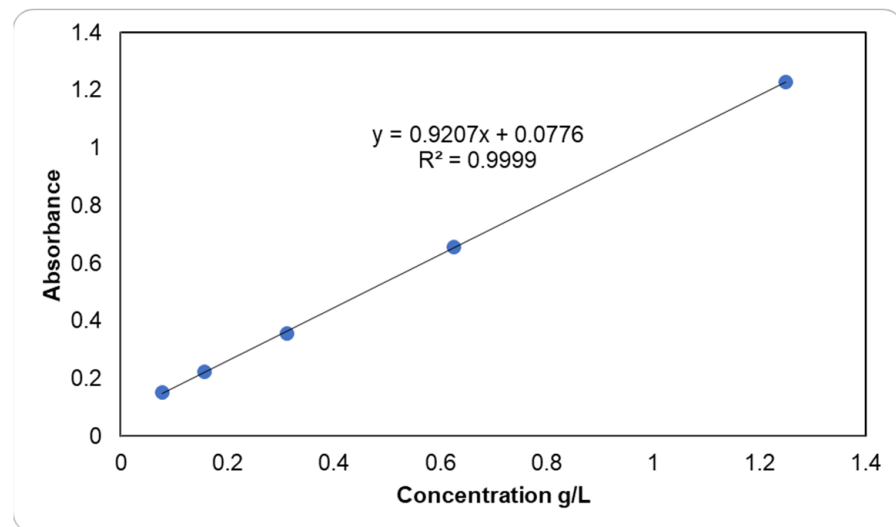


Figure 2. The calibration curve for benzalkonium chloride.

The calibration curve at 262 nm has the following equation:

$$y = 0.9207 * X + 0.0776 \dots \quad (1)$$

and an R^2 value = 0.9999.

The BAC exhaustion percentage was also calculated from the absorbance value using the following formula:

$$\% E = (A_0 - A_t) / A_0 * 100 \quad (2)$$

where A_0 = absorbance of stock solution and A_t = absorbance of filtered solution after the exhaustion for a given time [33].

2.3. Statistical Analysis

The data were analyzed using one-way ANOVA with Tukey's pairwise comparisons tests. The values are reported as means \pm StDev, $n = 3$. Different superscript letters for specific attributes indicate significant mean differences, $p < 0.05$.

3. Results and Discussion

The different physical properties of the wood, non-wood, and textile fibers were evaluated by measuring fiber length, coarseness, density, and fines of the fibers, as shown in Table 1. Visual and microscopic images of the different wipes were taken to visualize their morphology, as shown in Figure 3.

Table 1. Characterizations of wood, non-wood, and textile fibers.

| Wood and Non-Wood Fibers | | | | Textile Fibers | | |
|--------------------------|--------------------------|--|------------------|-----------------|--------------------|-------------------------|
| Fiber Type | Fiber Length, l_w (mm) | Coarseness ($\text{mg}\cdot\text{m}^{-1}$) | Fines (%) | Fiber Type | Staple Length (mm) | Linear Density (Denier) |
| Hardwood | 1.15 ± 0.081 | 0.10 ± 0.009 | 20.58 ± 1.85 | Greige Cotton | 30.25 ± 2.72 | 1.75 ± 0.16 |
| Softwood | 2.24 ± 0.180 | 0.17 ± 0.015 | 21.97 ± 1.76 | Bleached Cotton | 23.21 ± 1.86 | 1.08 ± 0.68 |
| BEK | 0.79 ± 0.047 | 0.08 ± 0.005 | 9.50 ± 0.57 | Viscose | 26.45 ± 1.59 | 2.21 ± 0.14 |
| Hemp Kraft | 0.74 ± 0.052 | 0.15 ± 0.011 | 17.20 ± 1.20 | Tencel | 42.54 ± 2.97 | 1.42 ± 0.10 |
| Hemp Carbonate | 0.67 ± 0.054 | 0.22 ± 0.018 | 11.20 ± 0.89 | Polyester | 51.00 ± 4.08 | 0.95 ± 0.67 |

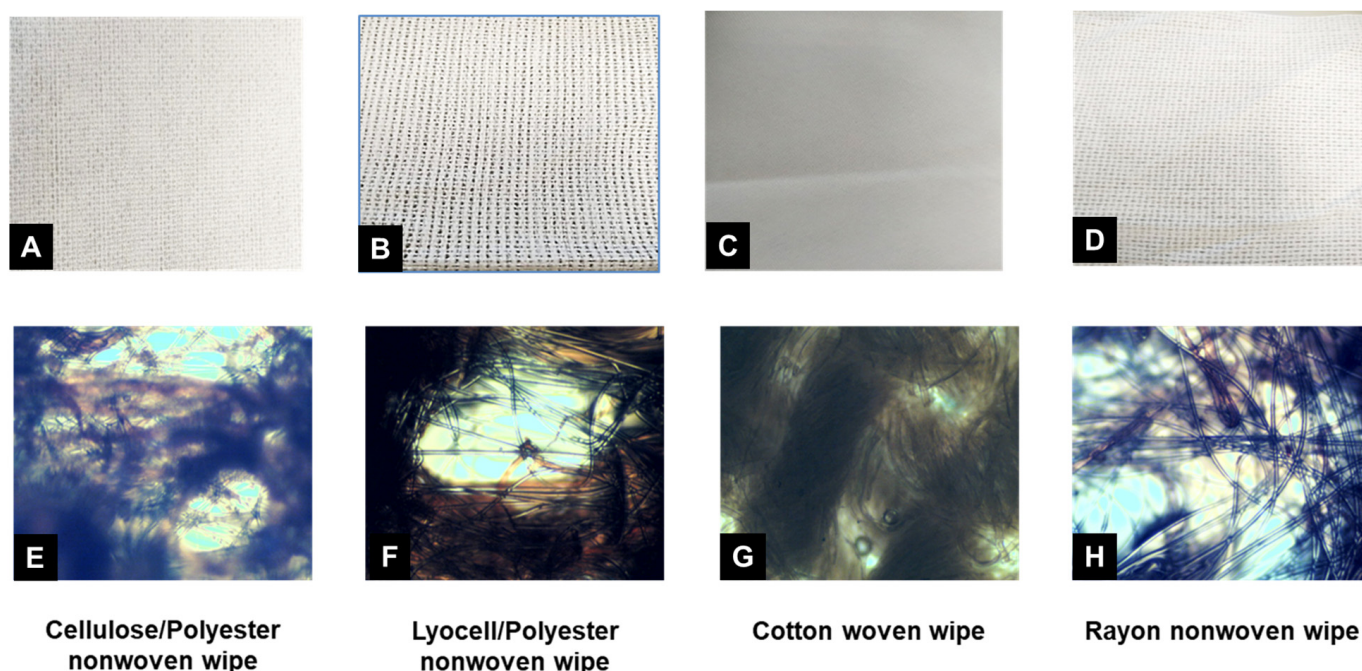


Figure 3. Actual images (A–D) of the wipes (top) and microscopic images (E–H) of wipe surface structures (bottom).

It can be seen from Figure 3 that the non-woven wipes have a more porous structure than the woven cotton wipes, which may affect the absorptive capacity of the product, as shown in Table 2. The other physical properties of the commercial wipes, such as their construction, thickness, basis weight, along with their absorptive capacity, are shown in Table 2. The cellulose–polyester blend has greater absorbency than pure cotton, which may be due to the construction of the wipes. The pure cotton wipes produced at higher

grammage are denser than the blend, which reduces the absorptive capacity of the pure cotton wipe, and the absorptive capacity of rayon is slightly higher than cotton due to its lower crystalline structure [34].

Table 2. Characterizations of wipes.

| Material | Construction | Thickness (μm) | GSM (g/m^2) | Absorbent Capacity (mL/m^2) |
|---------------------------------------|------------------------------|-----------------------------|-------------------------------|---|
| 50% Cellulose/ 50% Polyester blend | Hydroentangled, nonwoven | 575 ± 23.81 | 56.9 ± 2.5 | 344 ± 8.26 |
| 58% Polyester/ 42% Lyocell | Hydroentangled, apertured | 769.5 ± 38.47 | 74.4 ± 4.83 | 395 ± 17.77 |
| 100% Cotton | 2×1 twill woven | 435.25 ± 26.11 | 183.1 ± 5.29 | 300 ± 10.8 |
| 100% Rayon | Spunbond, nonwoven | 748.75 ± 26.21 | 71.99 ± 3.59 | 328 ± 8.2 |

The chemical structures of the different textile, wood, and non-wood fibers were analyzed via FTIR, as shown in Figure 4. The appearance of a peak in the region of 1030 cm^{-1} is due to C-O-C hydroxide groups in the carbohydrates. The peaks at 1240 cm^{-1} may be due to an aromatic ester compound. The peak corresponding to 1750 cm^{-1} is from unconjugated C-O stretching, which is due to the vibrations of aliphatic carboxylic acids and ketones of hemicellulose. Moreover, the hydrogen-bonded stretching bands of the OH groups at 3400 cm^{-1} is a characteristic peak of the hydroxyl groups in cellulose [35]. All of the fibers showed similar FTIR spectra since they possessed lignocellulosic compositions, and their origins did not result in differences in their chemical structures.

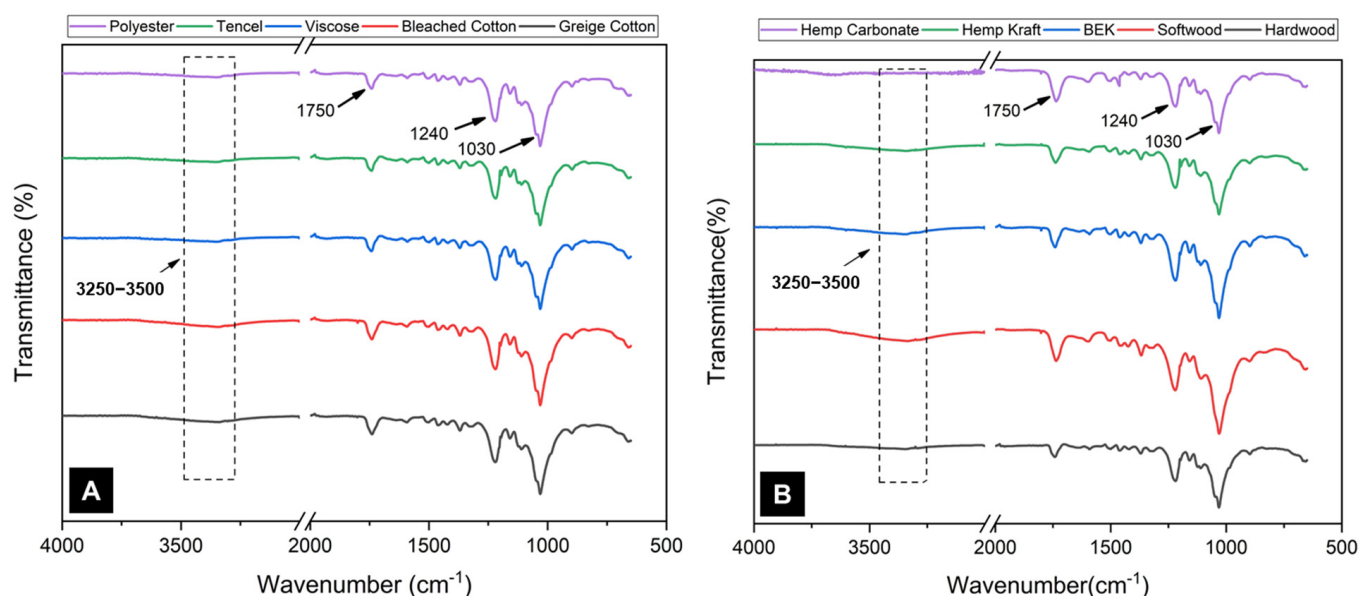


Figure 4. FTIR spectra of different (A) textile fibers and (B) wood and non-wood fibers.

The polyelectrolyte adsorption technique using high molecular weight poly-DADMAC was used to quantitatively measure fiber surface charge because these polymers could not penetrate the porous fiber. Fiber surface charge is a significant characteristic of cellulose fibers, which strongly affect their adsorption and exhaustion properties. The cellulosic fiber charge correlates to the number of anionic functional groups. The numbers of these functional groups, including carboxyl, sulfonic acid, and ionizable hydroxyl groups, vary with cellulose fiber origin and chemical treatment, such as bleaching, scouring, and physical modification [25]. When any fiber is immersed in water, this creates anionic charges on its

surface. Figure 5A shows data for textile fiber, and Figure 5B shows data for wood and non-wood fibers. A graph is plotted for every fiber to indicate the change in streaming potential as titration proceeds. Greige cotton fiber has maximum streaming potential, i.e., -1800 mV, and requires 0.2 mL of titrant volume to make the streaming potential zero. The streaming potential is a significant characteristic of cellulose fibers, which correlates to the number of anionic functional groups, and strongly affects the adsorption properties of the fibers. Synthetic fiber has minimum initial streaming potential, and required a minimum amount of cationic titrant to achieve zero streaming potential. For all of the other cellulosic fibers, the cationic volume demand lies between greige cotton and polyester.

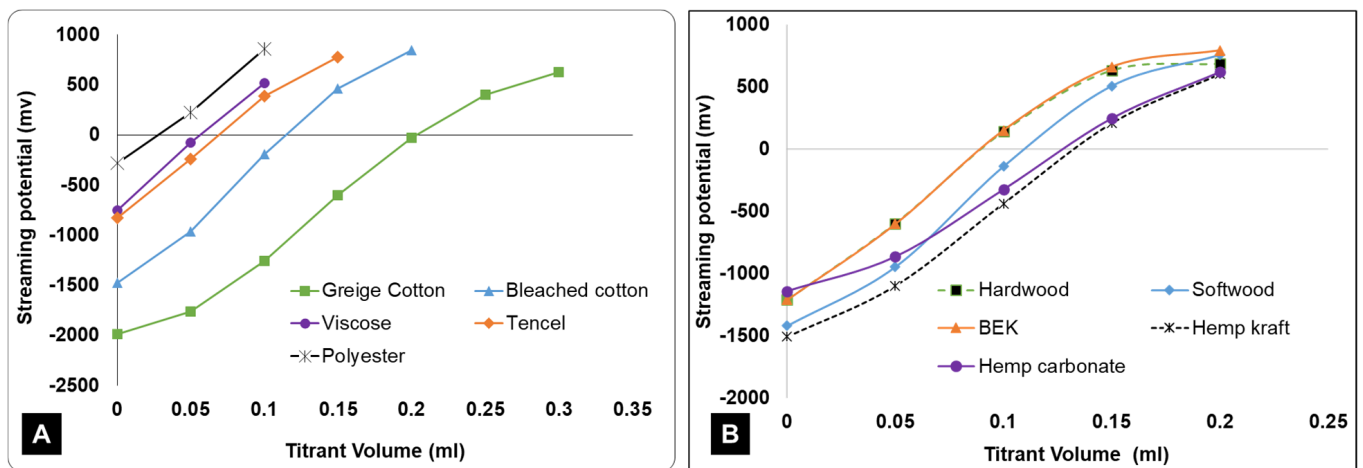


Figure 5. Streaming potential of (A) textile fibers and (B) wood and non-wood fibers.

The cationic volume requirement is related to the surface charge density, where the latter can vary depending on the source of the fiber and processing parameters. From Figure 6A, it can be observed that the surface charge density for greige cotton is the highest, and it is 1.8 times that of bleached cotton. The difference in surface charge density for the greige and bleached cotton is because of their different chemical compositions and physical properties. Cotton fiber has a fibrillar structure that consists of a primary wall, secondary walls, and lumen. The outer layer has the most non-cellulosic material, including wax, pectin, and proteinaceous material [15]. Pectin is a complex polysaccharide that has a $-\text{COOH}$ group that leads to an increase in the functional groups available on the surface, which results in cotton fiber's high surface charge density. In the case of bleached cotton, the bleaching process removes the wax as well as the pectic and other functional groups, leaving a surface with only cellulosic $-\text{OH}$ groups, and resulting in less surface charge and a lower absorptive capacity for bleached cotton than greige cotton. Softwood fibers have a greater surface charge density than hardwood fibers, as shown in Figure 6B, which could be due to the higher carboxyl content that comes from the conversion of 4-O-methylglucuronic acid side groups (MeGlcA) of xylan to hexenuronic acids (HexA) during pulping [25]. Physical properties and the chemical composition affect the surface charges and thus, BEK has a greater surface charge density compared to hardwood fibers due to the presence of more carboxyl groups [25]. Hemp carbonate has a relatively higher carboxyl content and surface charge than hemp kraft due to the presence of more carboxyl groups on its surface [25]. Viscose and Tencel have the same chemical composition, but they are manufactured using a different chemical, which affects the morphological structures of these fibers. Tencel is softer and more absorbent than viscose. The absorptive capacity of Tencel is slightly more than that of viscose. Polyester has the fewest surface charges, as this fiber has no functional groups on its surface. Its measured surface charge density is due to the presence of finishing oils used during manufacturing processes.

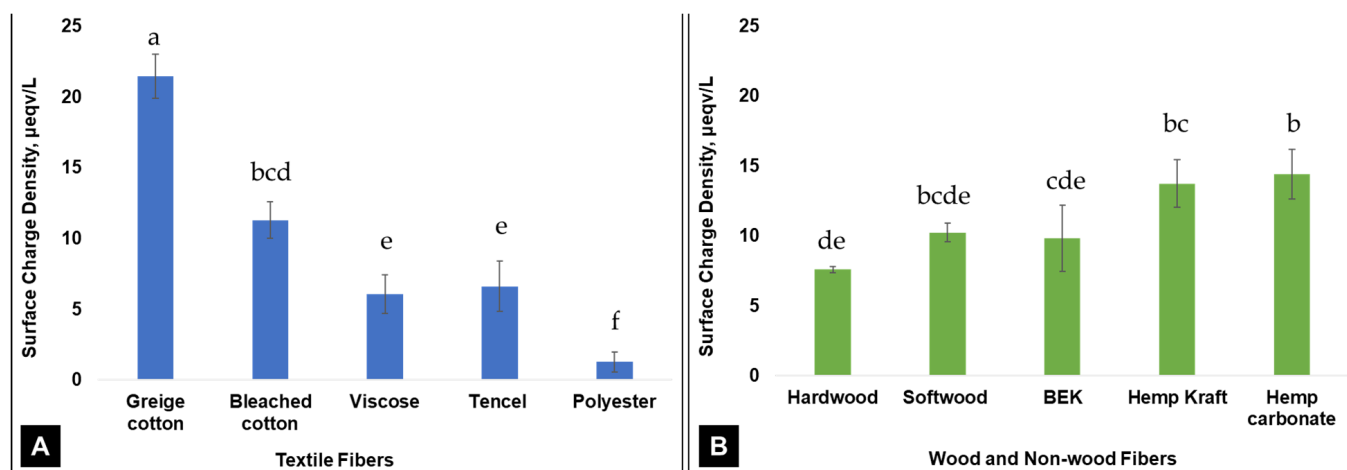


Figure 6. Surface charge densities ($\mu\text{eqv/L}$) of different (A) textile fibers and (B) wood and non-wood fibers. Data for textile and wood/non-wood fibers were analyzed together using one-way ANOVA with Tukey's pairwise comparisons tests. Values are means \pm StDev, $n = 3$. Different superscript letters (a, b, c, d, e, f) indicate significant mean differences, $p < 0.05$.

Cellulose-based fiber exhibits a negative surface charge when immersed in a neutral aqueous solution, as observed in Figure 6. Thus, the fibers in this study were expected to readily adsorb the positively charged benzalkonium chloride molecules from the bulk solution [33]. Since they absorb more BAC molecules, they could release a higher amount of BAC from the surface when centrifuged.

The surface morphology of fibers plays a crucial role in determining their functional properties, such as their absorbency, wettability, and exhaustion or desorption. SEM images of the wood, non-wood, and textile fibers were taken to observe how the morphology of the fibers affects the exhaustion of BAC from the different fibers (Figure 7). As wood and non-wood fibers are short, flat, and have hairy structures with large surface areas, they can absorb more BAC than the textile fibers since the hairy rough surface allows them to interact more with the BAC than the straight and smooth textile fibers. Therefore, the large surface area of these fibers can provide better and more controlled exhaustion of fluids, which can improve cleaning performance. Moreover, wood and non-wood fibers are renewable and sustainable resources that can be obtained from various sources, such as agricultural residues, recycled paper, and wood chips. Using these fibers as an alternative to textile fibers can reduce the dependence on non-renewable resources and minimize the environmental impact of the production and disposal of wipes and hygiene products.

Figure 8 shows the crystallinity indexes of the different fibers. The results showed that wood fibers have the highest degree of crystallinity, i.e., the cellulose crystallites in the natural fibers are more ordered and tightly packed than the crystallites of the textile and synthetic fibers. Tencel, viscose, and PET fibers showed much lower crystallinity index (CI). This may be due to the manufacturing processes used for these fibers, where the Tencel and viscose fibers are produced by treating with harsh chemicals and NaOH. The lower CI value of the PET fiber was due to the tacticity of the functional groups within the polymer structure, which lacks periodicity to induce higher crystallinity.

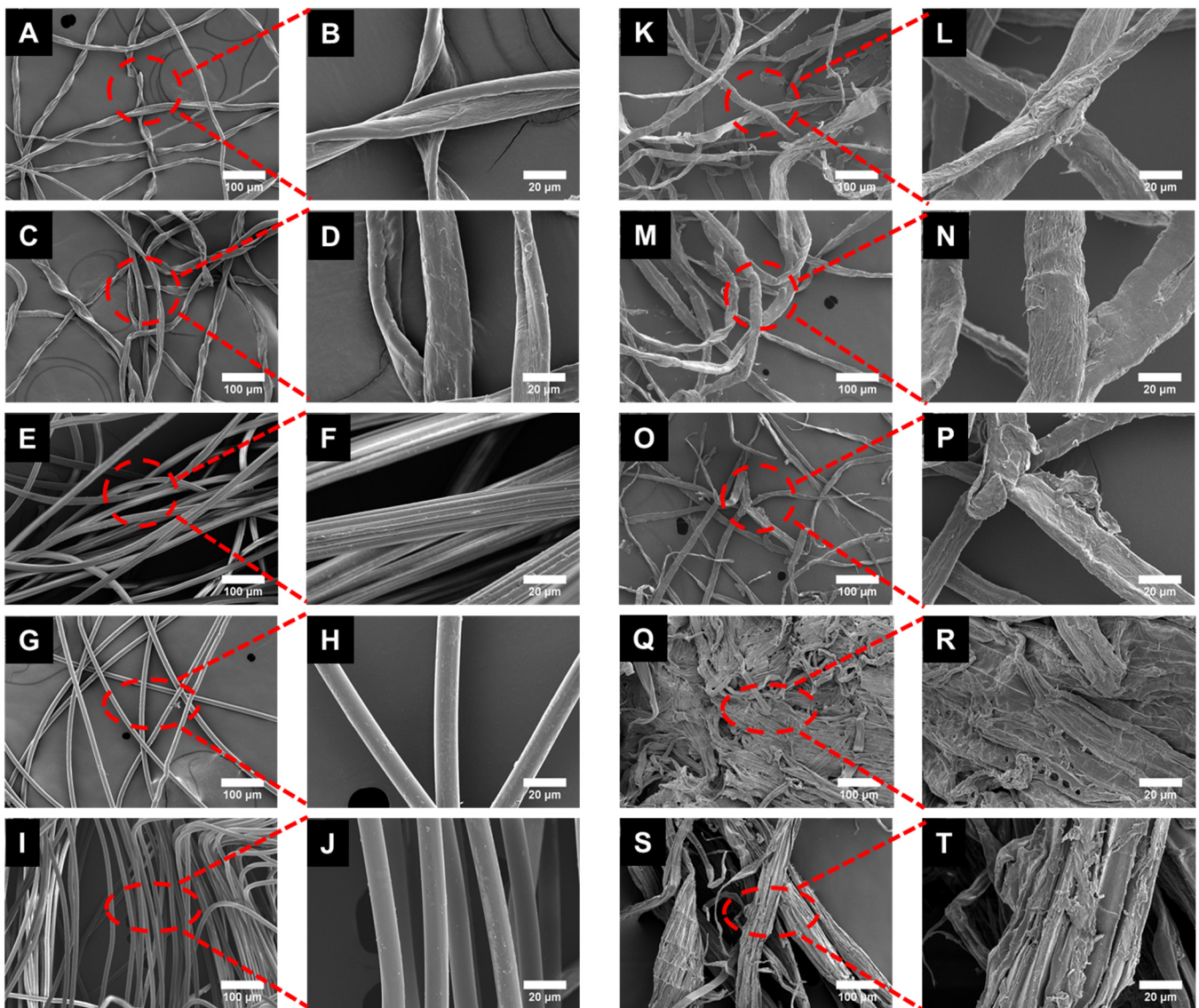


Figure 7. SEM images of different wood, non-wood fibers, and textile fibers: (A,B) GC, (C,D) BC, (E,F) viscose, (G,H) Tencel, (I,J) polyester, (K,L) HW, (M,N) SW, (O,P) BEK, (Q,R) hemp kraft, and (S,T) hemp carbonate.

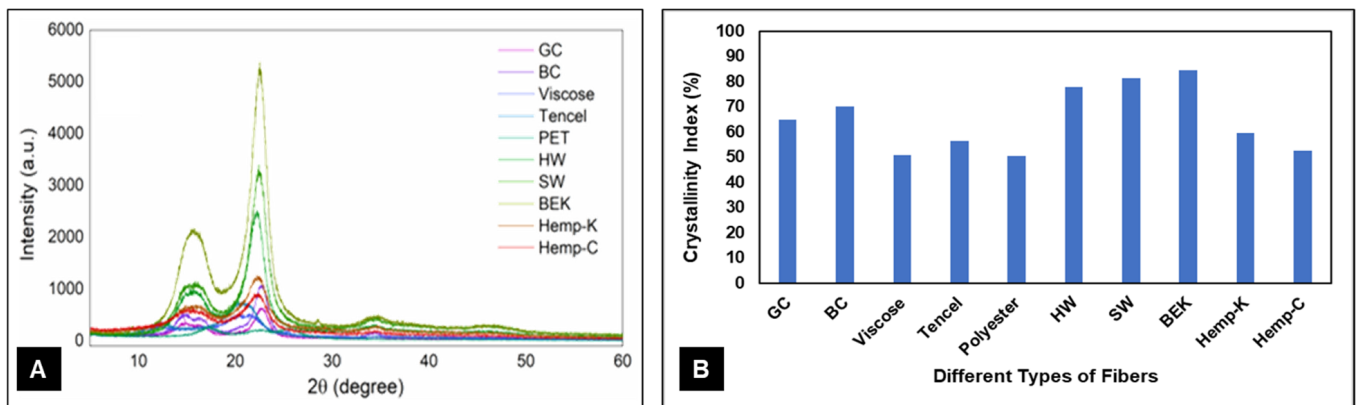


Figure 8. (A) XRD crystallography and (B) crystallinity index of different wood, non-wood, and textile fibers.

The lower CI value of the hemp fibers was due to presence of branched hemicelluloses, which induced a branched network through extensive crosslinking by cinnamate acid ester linkages and hydrogen bonding. The hemp kraft showed a higher CI since it was carried out at a higher pH, which dissolved more amorphous cellulose than the carbonate process that operated at a lower pH [25]. The higher CI of the wood fibers resulted in better exhaustion due to controlled absorption of the BAC onto the fibers, unlike the fibers with lower CI values, which might lead to irregular absorption of BAC.

The percentage exhaustion of the disinfectant solution from the different feedstock solutions was studied, as shown in Figure 9. Greige cotton adsorbs more BAC than bleached cotton due to its higher surface charge. Hence, it shows higher exhaustion of the disinfectant upon centrifuge. Viscose and Tencel are regenerated cellulose-based materials; they have the same chemical composition and the same surface charge density, but a difference in the manufacturing process affects their morphological structures. The cross-section is mainly influenced by the coagulation and spinning conditions, due to the use of a different solvent to dissolve the cellulose, which explains the slightly higher exhaustion for Tencel when compared to viscose. Softwood fibers have higher exhaustion compared to hardwood and BEK due to their higher specific surface area, longer fibers, higher fines content, and high surface charge density, which retain more BAC molecules. However, hardwood has higher exhaustion than BEK, which could be due to its higher fines content, allowing greater BAC adsorption onto SBHK fibers. Higher exhaustion by hemp carbonate fibers than hemp kraft also resulted from the higher adsorption of BAC molecules by hemp carbonate due to more carboxyl groups in the hemp carbonate fibers.

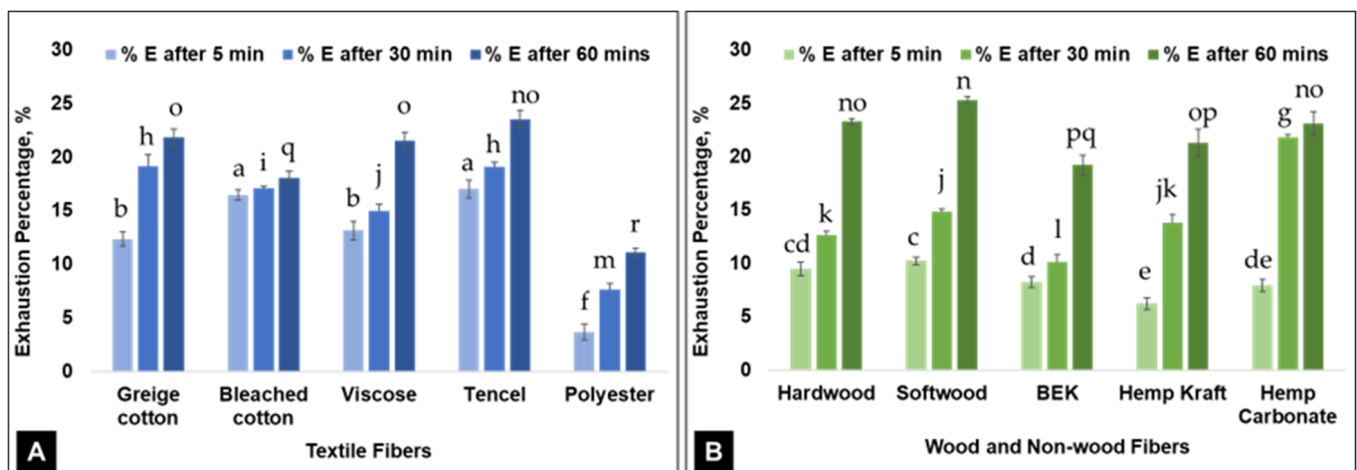


Figure 9. Percentage exhaustion of fibers at different time intervals for (A) textile fibers and (B) wood and non-wood fibers, where the concentration of the disinfectant solution is 0.625 g/L. Data for textile and wood/non-wood fibers were analyzed together via one-way ANOVA with Tukey's pairwise comparisons tests. Values are means \pm StDev, $n = 3$. Different superscript letters (%E after 5 min—a, b, c, d, e, f; %E after 30 min—g, h, i, j, k, l, m; and %E after 60 min—n, o, p, q, r) indicate significant mean differences, $p < 0.05$.

The exhaustion of the BACs onto the fibers depends on different factors, namely the chemical composition, surface charge density, concentration of the solution, and the immersion time of the fiber into the BAC solution. Figure 9 also shows the effect of time on the percentage exhaustion, as the data were taken for three different time intervals. As the time increased from 5 min to 60 min, the BAC exhaustion percentage increased. For textile-based cellulosic fiber, the BAC exhausted rapidly when the immersion time was 5 min, and was close to exhaustion after 30 min immersion time. However, at 60 min of immersion in the disinfectant, the total exhaustion percentage increased by a very small amount. The higher rate of exhaustion for textile cellulosic fiber was due to presence of more cellulose chains than the wood fibers, which allows more hydroxyls to be available

for BAC adsorption, and it was consequently followed by exhaustion [36]. Whereas the wood and non-wood cellulosic fibers have a lower exhaustion percentage at the beginning, the exhaustion increased with increased immersion time. It took longer for the wood and non-wood fibers to exhaust BAC from the solution onto the fiber surface than the textile fibers. For the textile fibers, greige cotton exhausted more BAC in comparison to bleached cotton for any given time, since greige cotton can adsorb more BAC molecules due to its higher surface charge density than bleached cotton. Tencel also resulted in higher exhaustion of BAC than viscose fibers for the same reason. Polyester fiber shows the lowest exhaustion, as they have a very low surface charge density without functional anionic groups on their surface that retain more disinfectant. Therefore, the bioavailability of the BAC was higher for the wood- and non-wood-based fibers compared to the textile fibers.

The effect of the initial BAC concentration, another important factor, on the amount of disinfectant exhausted, was also studied for 60 min at two different solution concentrations, 0.625 g/L and 1.25 g/L. The exhaustion of BAC did not increase with increased initial concentration; rather, the total amount of BAC exhausted decreased with increased concentrations of BAC (Figure 10). This may have occurred due to decreased numbers of BAC molecules adsorbed by the fiber surface from the formation of CMC (critical micelle concentration), where micelles started to form at 1.02 g/L [33]. The polyester showed the lowest exhaustion at both the concentrations, which can be observed in Figure 9 where the percentage exhaustion with respect to time was the lowest for polyester. The hemp carbonate showed the highest exhaustion percentage at both concentrations, which is coherent with the data of Figure 9 showing the highest exhaustion of hemp carbonate after 30 and 60 min.

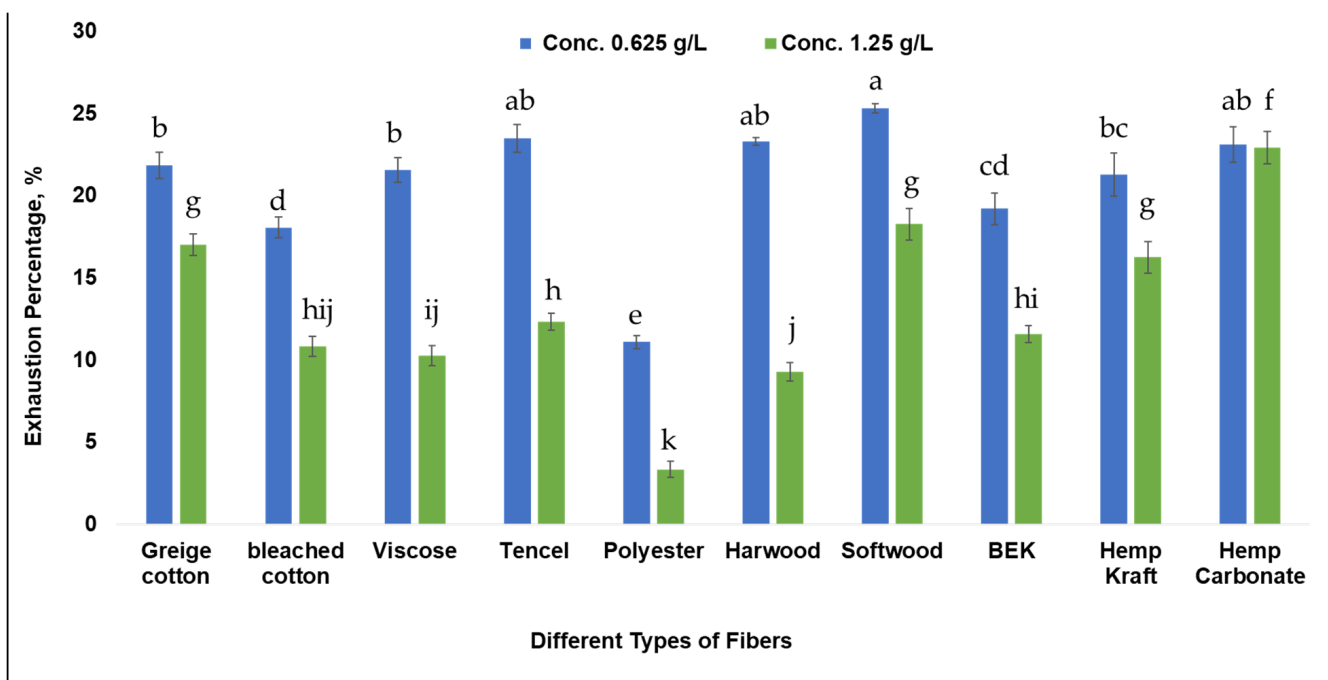


Figure 10. Exhaustion percentages for different fibers for two different concentrations at constant time. Data for textile and wood/non-wood fibers were analyzed together via one-way ANOVA with Tukey's pairwise comparisons tests. Values are means \pm StDev, $n = 3$. Different superscript letters (conc. 0.625 g/L—*a, b, c, d, e*; conc. 1.25 g/L—*f, g, h, i, j, k*) indicate significant mean differences, $p < 0.05$.

The exhaustion of BAC on the wipes was also investigated for two different time intervals, as shown in Figure 11A. It was observed from the statistical analysis that for non-woven cellulose/polyester and 100% rayon wipes, exhaustion is almost the same after 30 and 60 min (average % exhaustion is 8.5%); meanwhile, wipes made from lyocell/polyester

have the highest exhaustion value, and those made from 100% woven cotton have large differences in exhaustion percentages (almost double) after 30 and 60 min of 3.7% and 7.0%, respectively. In the case of nonwoven wipes, the exhaustion was fast because of the nonwoven fabric structure, which is an open structure having less grammage and fewer pores, resulting in a more open site for interaction with disinfectant cations. On the other hand, 100% woven cotton wipes have high grammage and low porosity, resulting in a smaller accessible surface area for interaction with cationic surfactant molecules. The wipes made of 100% rayon wipes showed almost the same exhaustion after 30 and 60 min, i.e., rayon became saturated very fast due to its lower crystallinity. Nonwoven wipes made from lyocell/polyester have the highest exhaustion percentage compared to all of the other nonwoven wipes due to fabric construction, which has a more open space and more available surface area for BAC to become attached onto.

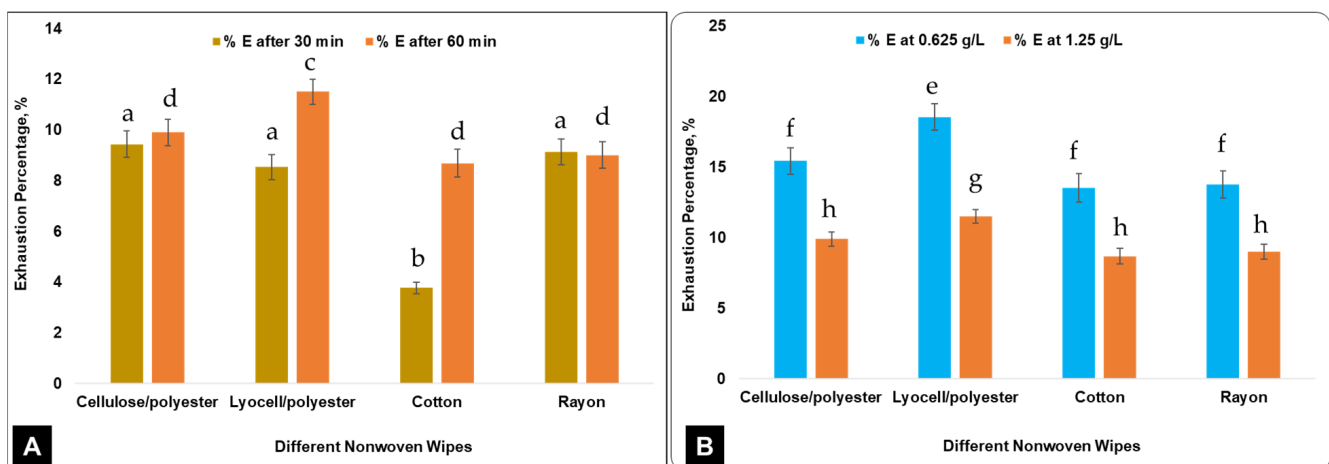


Figure 11. Exhaustion percentages for nonwoven wipes for (A) different times and (B) different concentrations of disinfectant after 60 min. Data for textile and wood/non-wood fibers were analyzed together via one-way ANOVA with Tukey's pairwise comparisons tests. Values are means \pm StDev, $n = 3$. Different superscript letters (%E after 30 min—*a, b*; %E after 60 min—*c, d*; %E at 0.625 g/L—*e, f*; and %E at 1.25 g/L—*g, h*) indicate significant mean differences, $p < 0.05$.

It is also observed from Figure 11B that as the concentration of disinfectant increased, the percentage exhaustion for all of the wipes decreased by almost 40% when the concentration was changed from 0.625 g/L to 1.25 g/L. However, the wipes made from lyocell/polyester still showed the highest exhaustion value at both of the concentrations. The total exhaustion of the disinfectant from the wipes at different time intervals and different concentration was lower than that of the textile fibers, which might be due to the change in morphological structure.

4. Conclusions

Lignocellulose has emerged as a sustainable and renewable biomaterial for its good absorbency, strength, cleaning properties, and biodegradable properties. In this research, different textile, synthetic, wood, and non-wood fibers were prepared, and their exhaustion capacities for benzalkonium chloride were measured and compared to that of the commercially available wipes on the market. It was found from the study that the wood and non-wood fibers showed lower exhaustion than the textile fibers. The immersion time also increased the percentage of the total exhaustion of BACs on the fibers. The exhaustion of BAC by the commercially available wipes was also investigated at different immersion times and concentrations of BAC. It was observed that the change in immersion time did not affect the exhaustion of cotton/polyester and rayon; however, the exhaustion for lyocell/polyester and cotton increased almost by 50% and 100%, respectively, when the immersion time was increased from 30 to 60 min. Furthermore, the exhaustion decreased

at higher concentrations of BAC. It was observed that commercial wipes, when prepared from the textile fibers, showed lower exhaustion, resulting in higher bioavailability of BAC. Therefore, wood and non-wood cellulosic fibers could be considered as a potential alternative option for renewable and sustainable wipes and hygiene products to meet the future demand.

Author Contributions: All authors contributed to the study conception and design. Material preparation, data collection, and analysis were performed by M.M., K.S.S., R.S. and S.A. The first draft of the manuscript was written by M.M. and K.S.S., and all authors commented on previous versions of the manuscript. M.M. and K.S.S. equally contributed to the manuscript. All authors have read and agreed to the published version of the manuscript.

Funding: The contributions of Lokendra Pal are in part supported by the E. J. “Woody” Rice Professorship Endowment 679385-20220.

Informed Consent Statement: Not applicable.

Data Availability Statement: Data are contained within the article.

Acknowledgments: This research was performed in part at the Analytical Instrumentation Facility (AIF) at North Carolina State University, which is supported by the State of North Carolina and the National Science Foundation (award number ECCS-2025064). This research made use of instrumentation at AIF, acquired with support from the National Science Foundation (DMR-1726294). The AIF is a member of the North Carolina Research Triangle Nanotechnology Network (RTNN), a site in the National Nanotechnology Coordinated Infrastructure (NNCI).

Conflicts of Interest: The authors have no competing interests as defined by Springer, or other interests that might be perceived to influence the results and/or discussion reported in this paper.

References

- Zhang, D. 6—Nonwovens for Consumer and Industrial Wipes. In *Applications of Nonwovens in Technical Textiles*; Chapman, R.A., Ed.; Woodhead Publishing Series in Textiles; Woodhead Publishing: Cambridge, UK, 2010; pp. 103–119. ISBN 978-1-84569-437-1.
- Baccouch, W.; Ghith, A.; Yalcin-Enis, I.; Sezgin, H.; Miled, W.; Legrand, X.; Faten, F. Investigation of the Mechanical, Thermal, and Acoustical Behaviors of Cotton, Polyester, and Cotton/Polyester Nonwoven Wastes Reinforced Epoxy Composites. *J. Ind. Text.* **2022**, *51*, 876–899. [[CrossRef](#)]
- Beesoon, S.; Behary, N.; Perwuelz, A. Universal Masking during COVID-19 Pandemic: Can Textile Engineering Help Public Health? Narrative Review of the Evidence. *Prev. Med.* **2020**, *139*, 106236. [[CrossRef](#)]
- Smithers Report Tracks Market Boom for Nonwoven Wipes. Available online: https://www.nonwovens-industry.com/contents/view_breaking-news/2020-12-01/smithers-report-tracks-market-boom-for-nonwoven-wipes (accessed on 1 September 2023).
- Nam, S.; Slopek, R.; Wolf, D.; Warnock, M.; Condon, B.D.; Sawhney, P.; Gbur, E.; Reynolds, M.; Allen, C. Comparison of Biodegradation of Low-Weight Hydroentangled Raw Cotton Nonwoven Fabric and That of Commonly Used Disposable Nonwoven Fabrics in Aerobic Captina Silt Loam Soil. *Text. Res. J.* **2016**, *86*, 155–166. [[CrossRef](#)]
- Goswami, P.; O’Haire, T. 3—Developments in the Use of Green (Biodegradable), Recycled and Biopolymer Materials in Technical Nonwovens. In *Advances in Technical Nonwovens*; Kellie, G., Ed.; Woodhead Publishing Series in Textiles; Woodhead Publishing: Cambridge, UK, 2016; pp. 97–114. ISBN 978-0-08-100575-0.
- Salem, K.S.; Clayson, K.; Salas, M.; Haque, N.; Rao, R.; Agate, S.; Singh, A.; Levis, J.W.; Mittal, A.; Yarbrough, J.M.; et al. A Critical Review of Existing and Emerging Technologies and Systems to Optimize Solid Waste Management for Feedstocks and Energy Conversion. *Matter* **2023**, *6*, 3348–3377. [[CrossRef](#)]
- Ichim, M.; Filip, I.; Stelea, L.; Lisa, G.; Muresan, E.I. Recycling of Nonwoven Waste Resulting from the Manufacturing Process of Hemp Fiber-Reinforced Recycled Polypropylene Composites for Upholstered Furniture Products. *Sustainability* **2023**, *15*, 3635. [[CrossRef](#)]
- Cao, H.; Cobb, K.; Yatvitskiy, M.; Wolfe, M.; Shen, H. Textile and Product Development from End-of-Use Cotton Apparel: A Study to Reclaim Value from Waste. *Sustainability* **2022**, *14*, 8553. [[CrossRef](#)]
- Santos, A.S.; Ferreira, P.J.T.; Maloney, T. Bio-Based Materials for Nonwovens. *Cellulose* **2021**, *28*, 8939–8969. [[CrossRef](#)]
- Liu, M.; Ma, C.; Zhou, D.; Chen, S.; Zou, L.; Wang, H.; Wu, J. Hydrophobic, Breathable Cellulose Nonwoven Fabrics for Disposable Hygiene Applications. *Carbohydr. Polym.* **2022**, *288*, 119367. [[CrossRef](#)]
- Salem, K.S.; Jameel, H.; Lucia, L.; Pal, L. Sustainable High-Yield Lignocellulosic Fibers and Modification Technologies Educing Softness and Strength for Tissues and Hygiene Products for Global Health. *Mater. Today Sustain.* **2023**, *22*, 100342. [[CrossRef](#)]
- Divya, R.; Indumathi, T.R.; Venugopal, T.; Prakash, C. Investigation on Potential Application of Non-Wood Pulp for Hygiene Products as Absorbent Core Substantial. *Biomass Conv. Bioref.* **2023**, 1–6. [[CrossRef](#)]

14. Hamouda, T.; Ibrahim, H.M.; Kafafy, H.H.; Mashaly, H.M.; Mohamed, N.H.; Aly, N.M. Preparation of Cellulose-Based Wipes Treated with Antimicrobial and Antiviral Silver Nanoparticles as Novel Effective High-Performance Coronavirus Fighter. *Int. J. Biol. Macromol.* **2021**, *181*, 990–1002. [[CrossRef](#)] [[PubMed](#)]
15. Slopek, R.; Condon, B.; Sawhney, P.; Reynolds, M.; Allen, C. Effect of Cotton Pectin Content and Bioscouring on Alkyl-Dimethyl-Benzyl-Ammonium Chloride Adsorption. *Text. Res. J.* **2012**, *82*, 1743–1750. [[CrossRef](#)]
16. Song, X.; Vossebein, L.; Zille, A. Efficacy of Disinfectant-Impregnated Wipes Used for Surface Disinfection in Hospitals: A Review. *Antimicrob. Resist. Infect. Control* **2019**, *8*, 139. [[CrossRef](#)] [[PubMed](#)]
17. Hora, P.I.; Pati, S.G.; McNamara, P.J.; Arnold, W.A. Increased Use of Quaternary Ammonium Compounds during the SARS-CoV-2 Pandemic and Beyond: Consideration of Environmental Implications. *Environ. Sci. Technol. Lett.* **2020**, *7*, 622–631. [[CrossRef](#)] [[PubMed](#)]
18. Nunes, B.; Cagide, F.; Fernandes, C.; Borges, A.; Borges, F.; Simões, M. Efficacy of Novel Quaternary Ammonium and Phosphonium Salts Differing in Cation Type and Alkyl Chain Length against Antibiotic-Resistant *Staphylococcus Aureus*. *Int. J. Mol. Sci.* **2024**, *25*, 504. [[CrossRef](#)] [[PubMed](#)]
19. Shamsuri, A.A.; Jamil, S.N.A.M. Application of Quaternary Ammonium Compounds as Compatibilizers for Polymer Blends and Polymer Composites—A Concise Review. *Appl. Sci.* **2021**, *11*, 3167. [[CrossRef](#)]
20. Huang, K.; Fan, X.; Ashby, R.; Ngo, H. Structure-Activity Relationship of Antibacterial Bio-Based Epoxy Polymers Made from Phenolic Branched Fatty Acids. *Prog. Org. Coat.* **2021**, *155*, 106228. [[CrossRef](#)]
21. Wu, X.; Viner-Mozzini, Y.; Jia, Y.; Song, L.; Sukenik, A. Alkyltrimethylammonium (ATMA) Surfactants as Cyanocides—Effects on Photosynthesis and Growth of Cyanobacteria. *Chemosphere* **2021**, *274*, 129778. [[CrossRef](#)]
22. Frolov, N.A.; Fedoseeva, K.A.; Hansford, K.A.; Vereshchagin, A.N. Novel Phenyl-Based Bis-Quaternary Ammonium Compounds as Broad-Spectrum Biocides. *ChemMedChem* **2021**, *16*, 2954–2959. [[CrossRef](#)]
23. Vereshchagin, A.N.; Frolov, N.A.; Egorova, K.S.; Seitkalieva, M.M.; Ananikov, V.P. Quaternary Ammonium Compounds (QACs) and Ionic Liquids (ILs) as Biocides: From Simple Antiseptics to Tunable Antimicrobials. *Int. J. Mol. Sci.* **2021**, *22*, 6793. [[CrossRef](#)]
24. Jennings, M.C.; Minbirole, K.P.C.; Wuest, W.M. Quaternary Ammonium Compounds: An Antimicrobial Mainstay and Platform for Innovation to Address Bacterial Resistance. *ACS Infect. Dis.* **2015**, *1*, 288–303. [[CrossRef](#)]
25. Salem, K.S.; Naithani, V.; Jameel, H.; Lucia, L.A.; Pal, L. Lignocellulosic Fibers from Renewable Resources Using Green Chemistry for a Circular Economy. *Glob. Chall.* **2020**, *5*, 2000065. [[CrossRef](#)]
26. Pascoe, M.J.; Mandal, S.; Williams, O.A.; Maillard, J.-Y. Impact of Material Properties in Determining Quaternary Ammonium Compound Adsorption and Wipe Product Efficacy against Biofilms. *J. Hosp. Infect.* **2022**, *126*, 37–43. [[CrossRef](#)]
27. Bloß, R.; Meyer, S.; Kampf, G. Adsorption of Active Ingredients of Surface Disinfectants Depends on the Type of Fabric Used for Surface Treatment. *J. Hosp. Infect.* **2010**, *75*, 56–61. [[CrossRef](#)]
28. Slopek, R.; Condon, B.; Sawhney, P.; Reynolds, M.; Allen, C. Adsorption of Alkyl-Dimethyl-Benzyl-Ammonium Chloride on Differently Pretreated Non-Woven Cotton Substrates. *Text. Res. J.* **2011**, *81*, 1617–1624. [[CrossRef](#)]
29. Engelbrecht, K.; Ambrose, D.; Sifuentes, L.; Gerba, C.; Weart, I.; Koenig, D. Decreased Activity of Commercially Available Disinfectants Containing Quaternary Ammonium Compounds When Exposed to Cotton Towels. *Am. J. Infect. Control* **2013**, *41*, 908–911. [[CrossRef](#)] [[PubMed](#)]
30. Gupta, U.S.; Dhamarikar, M.; Dharkar, A.; Chaturvedi, S.; Tiwari, S.; Namdeo, R. Surface Modification of Banana Fiber: A Review. *Mater. Today Proc.* **2021**, *43*, 904–915. [[CrossRef](#)]
31. Yokota, S.; Tagawa, S.; Kondo, T. Facile Surface Modification of Amphiphilic Cellulose Nanofibrils Prepared by Aqueous Counter Collision. *Carbohydr. Polym.* **2021**, *255*, 117342. [[CrossRef](#)] [[PubMed](#)]
32. Samaher Salem, K.; Kumar Kasera, N.; Ashiqur Rahman, M.; Jameel, H.; Habibi, Y.; Eichhorn, S.J.; French, A.D.; Pal, L.; Lucia, L.A. Comparison and Assessment of Methods for Cellulose Crystallinity Determination. *Chem. Soc. Rev.* **2023**, *52*, 6417–6446. [[CrossRef](#)] [[PubMed](#)]
33. Hinchliffe, D.; Condon, B.; Madison, C.; Reynolds, M.; Hron, R. An Optimized Co-Formulation Minimized Quaternary Ammonium Compounds Adsorption onto Raw Cotton Disposable Disinfecting Wipes and Maintained Efficacy against Methicillin-Resistant *Staphylococcus Aureus*, Vancomycin-Resistant *Enterococcus Faecalis*, and *Pseudomonas Aeruginosa*. *Text. Res. J.* **2018**, *88*, 2329–2338. [[CrossRef](#)]
34. Zambrano, M.C.; Pawlak, J.J.; Daystar, J.; Ankeny, M.; Goller, C.C.; Venditti, R.A. Aerobic Biodegradation in Freshwater and Marine Environments of Textile Microfibers Generated in Clothes Laundering: Effects of Cellulose and Polyester-Based Microfibers on the Microbiome. *Mar. Pollut. Bull.* **2020**, *151*, 110826. [[CrossRef](#)] [[PubMed](#)]
35. Tanpichai, S.; Biswas, S.K.; Witayakran, S.; Yano, H. Water Hyacinth: A Sustainable Lignin-Poor Cellulose Source for the Production of Cellulose Nanofibers. *ACS Sustain. Chem. Eng.* **2019**, *7*, 18884–18893. [[CrossRef](#)]
36. Ansell, M.P.; Mwaikambo, L.Y. 2—The Structure of Cotton and Other Plant Fibres. In *Handbook of Textile Fibre Structure*; Eichhorn, S.J., Hearle, J.W.S., Jaffe, M., Kikutani, T., Eds.; Woodhead Publishing Series in Textiles; Woodhead Publishing: Cambridge, UK, 2009; Volume 2, pp. 62–94. ISBN 978-1-84569-730-3.

Disclaimer/Publisher’s Note: The statements, opinions and data contained in all publications are solely those of the individual author(s) and contributor(s) and not of MDPI and/or the editor(s). MDPI and/or the editor(s) disclaim responsibility for any injury to people or property resulting from any ideas, methods, instructions or products referred to in the content.